

## Article

# Methanogenesis from Mineral Carbonates, a Potential Indicator for Life on Mars

Richard M. Wormald<sup>1</sup>, Jeremy Hopwood<sup>1</sup>, Paul N. Humphreys<sup>1</sup> , William Mayes<sup>2</sup>, Helena I. Gomes<sup>2,3</sup>   
and Simon P. Rout<sup>1,\*</sup>

<sup>1</sup> Department of Biological and Geographical Sciences, University of Huddersfield, Huddersfield HD1 3DH, UK; r.m.wormald@hud.ac.uk (R.M.W.); j.d.hopwood@hud.ac.uk (J.H.); p.n.humphreys@hud.ac.uk (P.N.H.)

<sup>2</sup> Department of Geography, Geology and Environment, University of Hull, Hull HU6 7RX, UK; w.mayes@hull.ac.uk (W.M.); helena.gomes1@nottingham.ac.uk (H.I.G.)

<sup>3</sup> Food, Water, Waste Research Group, Faculty of Engineering, University of Nottingham, Nottingham NG7 2RD, UK

\* Correspondence: s.rout@hud.ac.uk

**Abstract:** Priorities for the exploration of Mars involve the identification and observation of biosignatures that indicate the existence of life on the planet. The atmosphere and composition of the sediments on Mars suggest suitability for anaerobic chemolithotrophic metabolism. Carbonates are often considered as morphological biosignatures, such as stromatolites, but have not been considered as potential electron acceptors. Within the present study, hydrogenotrophic methanogen enrichments were generated from sediments that had received significant quantities of lime from industrial processes (lime kiln/steel production). These enrichments were then supplemented with calcium carbonate powder or marble chips as a sole source of carbon. These microcosms saw a release of inorganic carbon into the liquid phase, which was subsequently removed, resulting in the generation of methane, with  $0.37 \pm 0.09$  mmoles of methane observed in the steel sediment enrichments supplemented with calcium carbonate powder. The steel sediment microcosms and lime sediments with carbonate powder enrichments were dominated by *Methanobacterium* sp., whilst the lime/marble enrichments were more diverse, containing varying proportions of *Methanomassiliicoccus*, *Methanoculleus* and *Methanosarcina* sp. In all microcosm experiments, acetic acid was detected in the liquid phase. Our results indicate that chemolithotrophic methanogenesis should be considered when determining biosignatures for life on Mars.

**Keywords:** methanogenesis; carbonate; biosignature



**Citation:** Wormald, R.M.; Hopwood, J.; Humphreys, P.N.; Mayes, W.; Gomes, H.I.; Rout, S.P. Methanogenesis from Mineral Carbonates, a Potential Indicator for Life on Mars. *Geosciences* **2022**, *12*, 138. <https://doi.org/10.3390/geosciences12030138>

Academic Editors: Christophe Dupraz, Pieter T. Visscher, Kimberley L Gallagher, Brendan Paul Burns, Michael Rogerson, Alberto G. Fairén and Jesus Martinez-Frias

Received: 6 December 2021

Accepted: 14 March 2022

Published: 16 March 2022

**Publisher's Note:** MDPI stays neutral with regard to jurisdictional claims in published maps and institutional affiliations.



**Copyright:** © 2022 by the authors. Licensee MDPI, Basel, Switzerland. This article is an open access article distributed under the terms and conditions of the Creative Commons Attribution (CC BY) license (<https://creativecommons.org/licenses/by/4.0/>).

## 1. Introduction

The search for evidence of life on Mars has been a priority in Mars exploration for a number of years [1]. This activity has focused on the analysis of the Martian environment for biosignatures, or signals that indicate the presence, or previous existence, of life [2] and has driven the development of a number of planetary investigations, including the Mars Rover [3], InSight [4] and ExoMars Missions [5].

It is recognised that the consistent detection of methane on Mars [6] may be an indication of either current or ancient microbial methanogenesis [7]. Methanogenesis proceeds by a number of routes [8], with hydrogenotrophy ( $4\text{H}_2 + \text{CO}_2 \rightarrow \text{CH}_4 + 2\text{H}_2\text{O}$ ) being identified as the most plausible Martian route [9] since it can proceed at the expense of molecular hydrogen generated by serpentinisation [10] and/or seismology [11]. Consequently, terrestrial serpentinisation systems have been identified as potential Martian analogues [12,13]. However, whilst serpentinisation does provide hydrogen, it is associated with alkaline conditions [12,14,15], which pose issues for hydrogenotrophic methanogens due to the reduction in available  $\text{CO}_2$  through carbonate precipitation.

Carbonates are of interest from a Martian perspective, since a warmer, wetter climate with a CO<sub>2</sub>-rich atmosphere was predicted during the Noachian epoch [16] and the mineral phases are likely to be an indicator of atmospheric evolution [17]. Carbonate deposits represent a potential Martian habitat [18] from which microbial communities could emerge through direct interactions with these deposits.

In the present study, we investigate the potential for hydrogenotrophic methanogens to generate methane in the presence of mineral carbonates at an alkaline pH. Enrichment cultures were prepared from the sediments of sites across the north of England that had received waste disposal from the lime kiln or steel industries. On interaction with ground and spring waters, there is hydrolysis, resulting in the formation of aqueous calcium hydroxide, which subsequently results in the formation of tufa following the dissolution of CO<sub>2</sub> [19]. These hydrogenotrophic enrichments were then sub-cultured to microcosms in which CO<sub>2</sub> was only available in the form of mineral carbonates.

## 2. Materials and Methods

### 2.1. Release of Dissolved Inorganic Carbon from Carbonate Sources

To determine the extent of the release of dissolved organic carbonate (DIC) at pH 10.0, 5 g of a carbonate source (calcium carbonate powder or marble chips with a granule size of 20–30 mm, both Fisher Scientific, Hampton, NH, USA) was added to basal medium (BM, Tables S1 and S2 and described in [20]). Liquid samples of BM were then taken every 7 days DIC, determined using a Shimadzu TOC5000A employing nitrogen as a carrier gas at a flow rate of 150 mL/min with sodium carbonate/sodium hydrogen carbonate standard solutions for calibration.

### 2.2. Sampling Sites and Preparation of Enrichment Cultures

Sediment samples were obtained from 13 sites comprising environments that had received lime because of quarrying, historical lime kiln operations, or steel slag from stainless steel production between 40 and ~350 years of age (Table S3 and described in [20]). The hydration of these waste forms leads to the formation of alkaline leachates (often pH > 11) that flow into nearby soils and waterbodies with little to no dilution. The evolution of these soils leads to them becoming a source of alkaliphilic and alkalitolerant microorganisms. Soil sediment cores were taken by removing the grass layer and upper layer (10–15 cm) of soil before the lower 5–10 cm of sediment was collected and used to fill a 50 mL sterile collection tube to exclude the headspace and sealed. To generate hydrogenotrophic enrichment cultures, 5 g of sediment was mixed with 5 mL of a BM (pH 10.0) before 5 mL of the slurry was added to a 100 mL bottle with 45 mL of the BM. All manipulations were carried out in an anaerobic chamber with a 10%/90% H<sub>2</sub>:N<sub>2</sub> atmosphere and bottles sealed immediately with a butyl rubber stopper. The enrichments were then incubated at 25 °C for 2 weeks in the dark before the headspace gas was analysed (see below) for the presence of methane gas. In the enrichments where methane was detected, they were sub-cultured by taking 5 mL of inoculum and adding it to 45 mL of fresh BM and regenerated headspace. Following the three subcultures, the resulting enrichment was used as a stock inoculum for the carbonate supplementation experiments. Throughout the preparation of the enrichment cultures, there was no addition of any organic carbon substrates, and the dilution factor associated with their preparation meant that any residual organic carbon from the soil matter was below the detection limits of the TOC analysis described below.

### 2.3. Reaction Set-Up and Analysis

Hydrogenotrophic methanogen enrichment cultures (5 mL) were added to 100 mL bottles in duplicate with 40 mL of BM and 5 g of either calcium carbonate powder or marble chips. Microcosms were prepared in an anaerobic chamber containing a 10%/90% H<sub>2</sub>:N<sub>2</sub> atmosphere and sealed with a rubber butyl stopper. The overall development of the microcosms is summarised in Figure S1. Apart from the microbial biomass, there

was no addition of organic carbon to any of the test or control reactions. As a control, in a second set of microcosms, the same set-up was established with 5 mL of culture replaced with uninoculated BM, a H<sub>2</sub>/N<sub>2</sub> headspace, and no added inorganic carbon source (calcium carbonate powder/marble chips). The sealed microcosms were incubated at 25 °C for 42 days in the dark and sampled every 7 days. Samples of headspace gas were analysed using an Agilent GC6850 equipped with a HP-PLOT/Q column with particle traps (35 m × 0.32 mm × 20 µm, Agilent Technologies, Cheadle, UK). A sample of the liquid phase (1 mL) was also taken from the microcosm and filtered through a 0.45 µm syringe filter. For the determination of dissolved inorganic carbon (DIC), a Shimadzu TOC5000A was used employing nitrogen as a carrier gas at a flow rate of 150 mL/min with DIC quantified against a sodium carbonate/sodium hydrogen carbonate standard. Volatile fatty acids present within the microcosms were determined through the addition of 1 part of sample to 9 parts of 85% *w/v* phosphoric acid and vortexing, before analysis by HP GC6890 under the operating conditions described in Rout et al. [21]. At the end of the 42 days of incubation, the microcosm fluid from each site was pooled for the extraction of nucleic acids. The samples were initially concentrated by centrifugation at 8000× *g* for 10 min, with 5 mL of the supernatant used to re-suspend the pellet. DNA was then extracted from the suspension following the method of Griffiths et al. [22]. The presence of DNA was confirmed through electrophoresis and quantified through a Qubit fluorometer. The V4 region of the Archaeal 16S rRNA gene was then sequenced from each community through Illumina Miseq Nano sequencing (ChunLab Inc., Seoul, Korea). The resulting reads were trimmed and quality-checked using an in-house protocol, and identifications were made by comparison with EZBioCloud. Non-metric multidimensional scaling (NMDS) analysis was carried out using the VEGAN package (<https://cran.r-project.org/web/packages/vegan/index.html>, last accessed on 10 March 2022) in R version 3.6.

### 3. Results

In the absence of a microbial inoculum, there was no evidence of methane generation (data not shown). These abiotic experiments did, however, result in the release of inorganic carbon into the liquid phase (Figure 1). The release of DIC was greater from the calcium carbonate powder, reaching  $4.6 \pm 0.7$  mmoles C compared with  $2.1 \pm 0.4$  mmoles C from the marble chips. Using PHREEQc analysis with the BM and calcium carbonate, the concentration of total calcium and DIC after equilibration with calcite at pH 10.0 was determined assuming a closed system. This suggested that, at pH 10 and equilibrium, any dissolved inorganic carbonate would be predominantly present as HCO<sub>3</sub><sup>−</sup> (61.6%) and CO<sub>3</sub><sup>2−</sup> (38.4%) over CO<sub>2</sub> (0.01%).

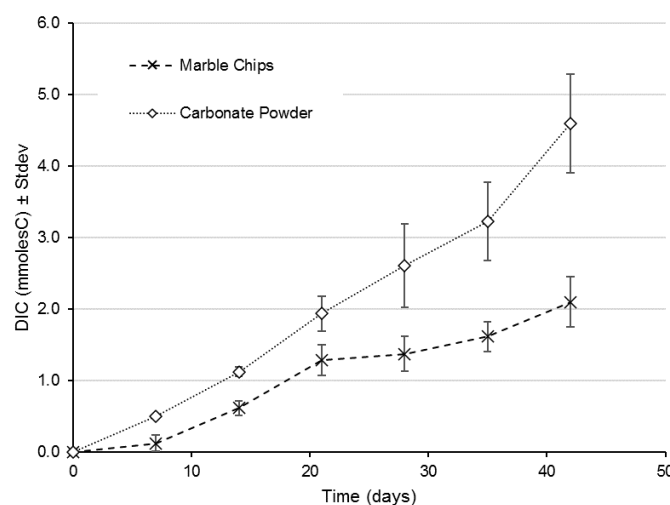


**Figure 1.** In abiotic reactions, there was evidence of the release of dissolved organic carbon into the reactor liquid phase from both marble chips and calcium carbonate powder.

Microcosms amended with calcium carbonate powder and the hydrogenotrophic methanogen enrichments from the lime and steel site sediments also saw the release of dissolved inorganic carbon within the liquid phase, which subsequently plateaued and fell following 14 days (lime) and 7 days (steel, Figure 2). Within the lime methanogen reactors amended with carbonate powder,  $0.31 \pm 0.03$  mmoles of methane were produced at the end of 42 days of incubation (Figure 2A), compared with  $0.37 \pm 0.08$  mmoles in those reactions with the steel methanogen inoculum (Figure 2B). Hydrogen was removed from the headspace from both reactor types. Within the microcosms amended with the marble chips, the generation of DIC, consumption of hydrogen headspace, and generation of methane were observed (Figure 2C,D). There was reduced generation of methane across the lime methanogen-inoculated reactions, with a mean production of  $0.17 \pm 0.02$  mmoles compared with  $0.31 \pm 0.09$  mmoles in those receiving the steel sediment methanogen inoculum (Table S4). Regardless of the carbonate source, the release of DIC into the liquid phase was observed within 14 days of incubation. Evidence of the consumption of the DIC was also observed across the different reaction types throughout the incubation period. Through headspace gas analysis, there was no evidence of carbon dioxide within the headspace of the microcosms.

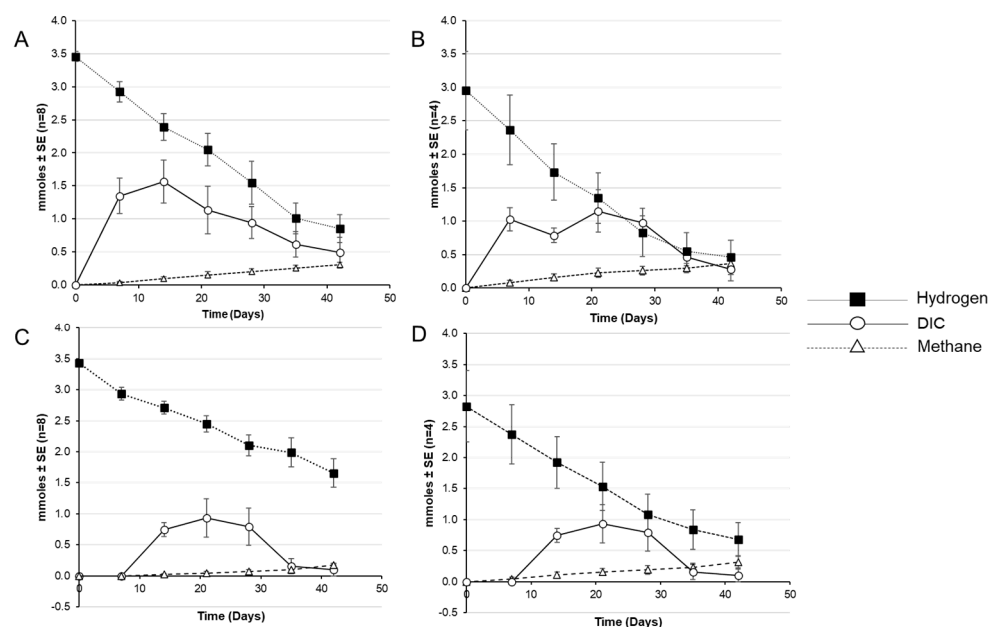


**Figure 2.** Consumption of hydrogen and generation of dissolved inorganic carbon/methane from calcium carbonate incubated with hydrogenotrophic enrichments from lime (A) and steel (B) sediments, or marble chips incubated with hydrogenotrophic enrichments from lime (C) and steel (D) sediments.

Overall, the microcosms utilising the lime enrichment of methanogens and supplemented with marble chips demonstrated both the lowest hydrogen consumption and methane generation rates (Figure 3). Microcosms that were prepared with methanogen enrichment from the steel site had greater than average methane generation rates, regardless of incubation with calcium carbonate powder or marble chips. With the exception of site SC, the hydrogen consumption rates were also above the average of the sample group. The lime methanogen enrichments that were supplemented with the calcium carbonate powder showed the greatest range of both the hydrogen consumption ( $37.0\text{--}75.1 \mu\text{mol/d}$ ) and methane generation ( $4.4\text{--}10.6 \mu\text{mol/d}$ ) rates. The stoichiometry of the reactors suggested that, although hydrogen was removed from the headspace and DIC from the liquid phase, these substrates were not diverted entirely to methane production (Table S5). This was further evidenced by the analysis of volatile fatty acids within the liquid phase, in which acetic acid was produced in both the lime and steel sediment enrichments supplemented

with either calcium carbonate powder or marble chips; however, no VFA were detected in the abiotic controls (Figure S2).

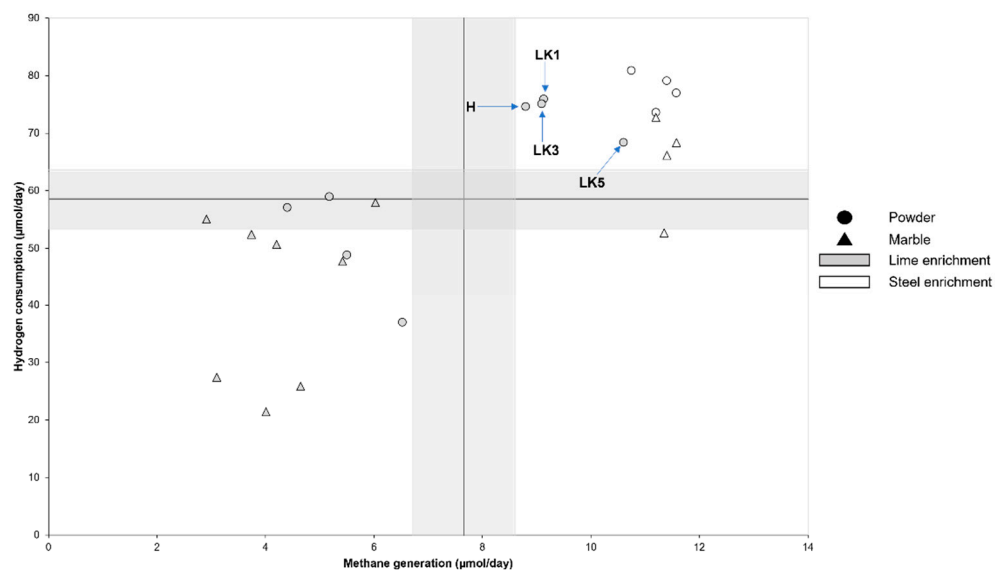


**Figure 3.** Comparison of hydrogen consumption and methane generation rates across the microcosms. Solid lines and grey area indicate the mean  $\pm$  SEM of the rates.

The enrichments from the lime kiln sites that were supplemented with calcium carbonate powder were dominated by taxa of the genus *Methanobacterium*, ranging from 57.1% in the community from the LK3 enrichment to 99.3% within the B enrichment (Figure 4). Within the lime samples supplemented with marble chips, the B enrichment was also dominated by *Methanobacterium* sp., representing 96.8% of the community profile, which contrasted with the other lime site sediment enrichments supplemented with marble chips. In the remaining marble chip enrichments, the communities of the T, LK1, LK3, and LK4 enrichments were composed largely of *Methanomassiliicoccus* (34.6–55.3%) and *Methanoculleus* sp. (42.1–54.1%). Communities from the H, LK2, LK3, and LK5 enrichments also contained *Methanosarcina* sp. within their communities (16.5–65.9%). The microcosm communities from the steel site enrichments were again dominated by *Methanobacterium* sp., whether supplemented with calcium carbonate powder or marble chips representing >86.8% of all the communities.

When supplemented with marble chips, the CS and RC communities also contained >10.9% *Methanocalculus* sp. NMDS analysis (Figure 5) of the Archaeal communities further illustrated the dissimilarity of the marble chip-supplemented lime enrichment communities in comparison to both the marble chip/steel and powder-supplemented communities from both sites. The lime site sediment enrichments that were supplemented with the marble chips contained more diverse communities than those supplemented with calcium carbonate powder, containing both a greater number of OTUs (Table S6) and Chao1 values (Figure S3).

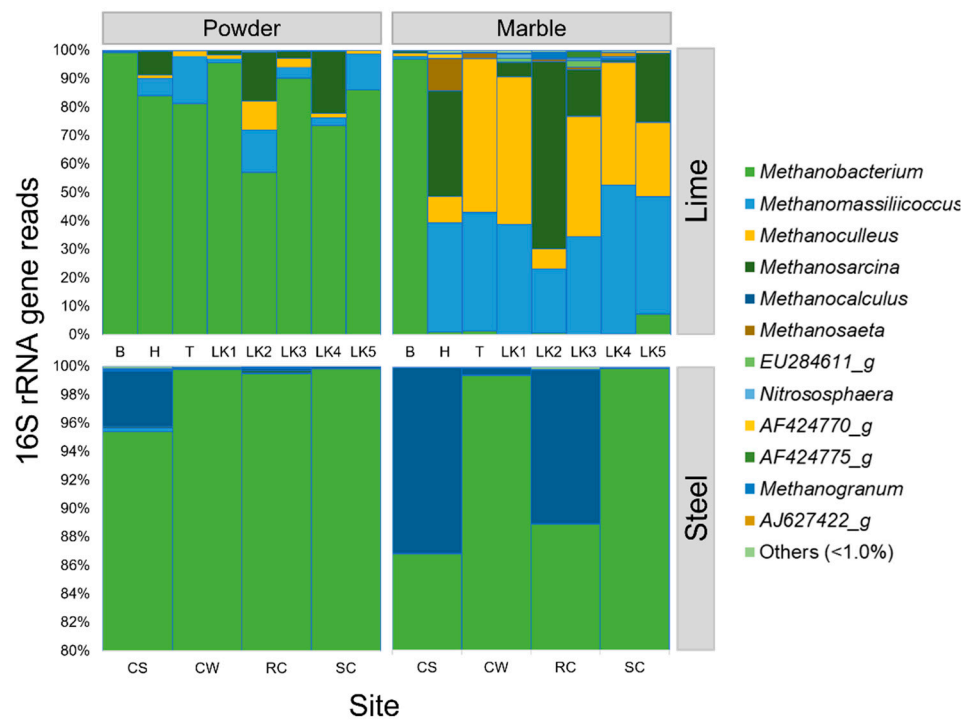


**Figure 4.** Community profiles of the microcosms that had been amended with either calcium carbonate powder or marble chips and supplemented with a lime site hydrogenotrophic methanogen enrichment or from a steel slag waste site.

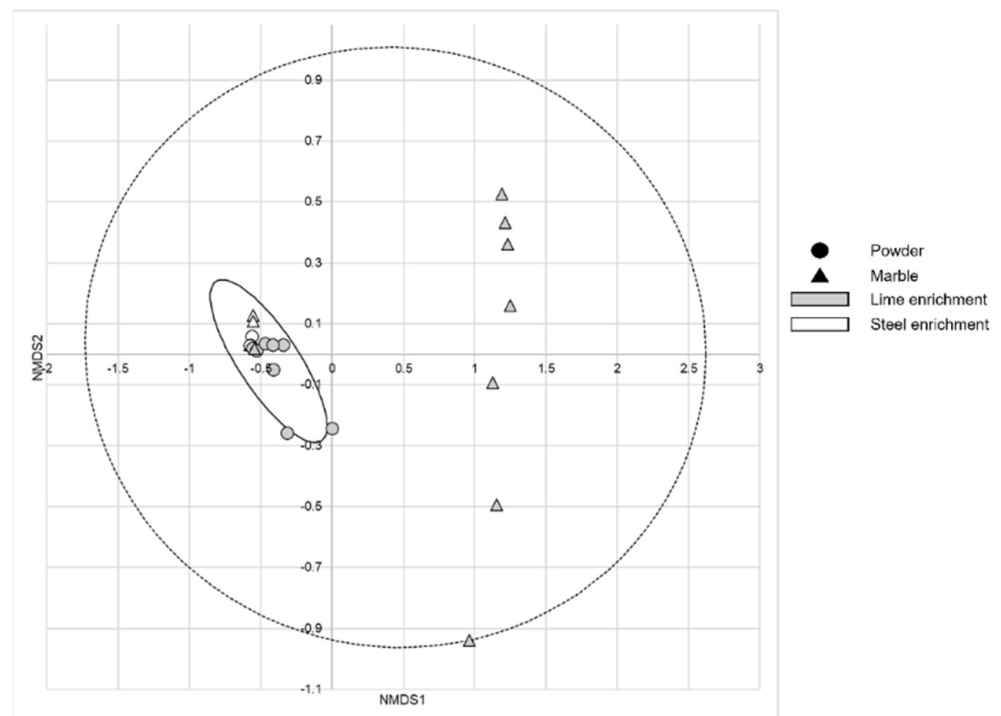


**Figure 5.** NMDS analysis illustrating the similarities between the steel site sediment enrichments supplemented with either calcium carbonate powder or marble chips and the lime site sediment enrichments supplemented with calcium carbonate powder. There was more dissimilarity between these sediments and the lime site sediment enrichments supplemented with the marble chips. Ellipses include all the sites within the NMDS based upon supplement (inner ellipse = powder) centred on the mean NMDS for those samples.

#### 4. Discussion

The data indicate that mineral carbonates can provide an electron acceptor in the presence of a hydrogen electron donor to facilitate methanogenesis. Whilst this was demonstrated previously with Ca and Mg carbonate powders at pH 6.9–8.4 with pure cultures of methanogens [23], the authors suggested that the organisms were utilising the small amounts of CO<sub>2</sub> released in equilibrium. The PHREEQC analysis indicated that, at elevated pH values, the carbon released from the soluble phase was more likely to be as a soluble carbonate or bicarbonate, and that methanogenic archaea could utilise this inorganic carbon as a CO<sub>2</sub> source for hydrogenotrophic methanogenesis. Although carbonates only represent ~2–5% of Martian dust, deposits of carbonate have been observed in environments such as the Jezero Crater/Syrtis–Terra Tyrrhena region [24,25] and could, therefore, represent a carbon source for utilisation by microorganisms within these niche environments. The release of carbon from the mineral phase does not appear to be a rate-limiting step for methanogenesis, since there was residual DIC present within the liquid phase. In addition, comparable rates of methane production when comparing the mineral forms within the steel site sediment enrichments were observed. There were, however, contrasting rates when comparing the mineral forms and lime enrichments.

The archaeal communities within both the steel and lime site sediment enrichments supplemented with calcium carbonate powder had similar profiles, dominated by *Methanobacterium* and *Methanomassiliicoccus* sp. Both these species are described as hydrogenotrophic within the literature [26–28]. Despite the similarities in the profiles of these communities observed by NMDS, there were differences in the methane generation and hydrogen consumption rates, particularly in the case of sites B, T, LK2, and LK4 enrichments; however, there was no correlation observed between these rates and the community profiles. In the lime site sediment enrichments supplemented with marble chips, there was an increased diversity of archaea. With the exception of the site B enrichment, there was a reduced presence of *Methanobacterium* sp., with increased detection of *Methanoculleus* and *Methanosarcina* sp. Whilst *Methanoculleus* sp. are described as hydrogenotrophic within the literature [29], *Methanosarcina* sp. are known to be more metabolically diverse, capable of acetoclastic, hydrogenotrophic and methylotrophic methane-producing metabolism [30]; however, the data here suggest that these genera present within the microcosms were unable to perform acetoclastic methanogenesis at pH 10.0. The absence of these species within the steel/marble microcosms may indicate that these taxa are not present within the in situ sediments. There was a production of acetic acid in all reactors, which may be a result of acetogens within the microbial communities. There is evidence to suggest that some methanogens can perform acetogenesis through a mechanism not dissimilar to the Wood–Ljungdahl pathway, acting as a carbon storage strategy [31,32], but this did not coincide with a subsequent removal, nor any enhancement to the methane generation rates within those associated microcosms. This suggests that elevated pH inhibits acetoclastic methanogenesis, and that *Methanosarcina* sp. observed in these reactions are contributing to hydrogenotrophic methanogenesis, which has been previously observed where alkaline soil communities were fed on hydrogen and carbon dioxide headspace [20].

Carbonate structures have been of interest from a Martian perspective as a morphological biosignature, in which it is expected that biological structures may entomb or preserve organisms, much like stromatolites [33,34]. Whilst these structures may be caused by biological activity, there may be potential for the formation of carbonates on the Martian surface due to serpentinisation events with mafic minerals in the subsurface, which also may generate hydrogen [12]. Overall, the data generated indicate that hydrogenotrophic methanogenesis should be considered as a potential biogenic route to methane in the Martian atmosphere.

**Supplementary Materials:** The following are available online at <https://www.mdpi.com/article/10.3390/geosciences12030138/s1>; Table S1: Mineral media composition per litre; Table S2: Trace element solution composition per litre. Table S3: Site locations and descriptions; Table S4: Mean

production of methane by soil and leachate type over 42 days of incubation; Table S5: Stoichiometric calculations of methane production and hydrogen consumption assuming the reduction of carbon dioxide to methane as  $\text{CO}_2 + 4 \text{H}_2 \rightarrow \text{CH}_4 + 2 \text{H}_2\text{O}$ ; Table S6: Number of OTUs observed within each microcosm Archaeal community; Figure S1: Overall scheme of microcosm development. In the control experiments, 5 mL of BM was added in place of 5 g of inoculum; Figure S2: The production of acetic acid was observed in microcosms, irrespective of lime/steel enrichment or carbonate supplement source; Figure S3: Chao1 values for the Archaeal communities present within the lime/steel and calcium carbonate powder/marble chip microcosms.

**Author Contributions:** Conceptualization, P.N.H., S.P.R., H.I.G. and W.M.; methodology, R.M.W. and S.P.R.; investigation, R.M.W.; resources, R.M.W. and H.I.G.; data curation, R.M.W., J.H. and S.P.R.; writing—original draft preparation, R.M.W. and S.P.R.; writing—review and editing, P.N.H., H.I.G., J.H. and W.M.; visualization, S.P.R.; supervision, P.N.H. All authors have read and agreed to the published version of the manuscript.

**Funding:** Richard Wormald’s PhD was supported by a Radioactive Waste Management Ltd. (RWM) research bursary. RWM Ltd. is a wholly owned subsidiary of the UK Nuclear Decommissioning Authority, a non-departmental public body which reports to the UK Department for Business, Energy, and Industrial Strategy. WM and HG were supported by the NERC R3AW grant (NE/L014211/1).

**Institutional Review Board Statement:** Not applicable.

**Informed Consent Statement:** Not applicable.

**Data Availability Statement:** The data presented in this study are available in the article and Supplementary Material.

**Acknowledgments:** We would like to thank the following individuals and organizations. David Johnson, for his assistance regarding the field kiln sites investigated. The Canal and River Boat Trust, Hanson Aggregates, Tarmac plc, Tee Valley Wildlife Trust and British Steel.

**Conflicts of Interest:** The authors declare that the research was conducted in the absence of any commercial or financial relationships that could be construed as a potential conflict of interest. RWM Ltd. had no influence on the design or execution of this study or the interpretation and reporting of the data reported in this paper.

## References

1. NASA. NASA Astrobiology Strategy 2015. Edited by L.Hays 2015. Available online: [https://nai.nasa.gov/media/medialibrary/2015/10/NASA\\_Astrobiology\\_Strategy\\_2015\\_151008.pdf](https://nai.nasa.gov/media/medialibrary/2015/10/NASA_Astrobiology_Strategy_2015_151008.pdf) (accessed on 8 November 2021).
2. Grenfell, J.L. A review of exoplanetary biosignatures. *Phys. Rep.* **2017**, *713*, 1–17. [[CrossRef](#)]
3. Williford, K.H.; Farley, K.A.; Stack, K.M.; Allwood, A.C.; Beaty, D.; Beegle, L.W.; Bhartia, R.; Brown, A.J.; de la Torre Juarez, M.; Hamran, S.-E. The NASA Mars 2020 rover mission and the search for extraterrestrial life. In *From Habitability to Life on Mars*; Elsevier: Amsterdam, The Netherlands, 2018; pp. 275–308.
4. Banerdt, W.B.; Smrekar, S.E.; Banfield, D.; Giardini, D.; Golombek, M.; Johnson, C.L.; Lognonné, P.; Spiga, A.; Spohn, T.; Perrin, C. Initial results from the InSight mission on Mars. *Nat. Geosci.* **2020**, *13*, 183–189. [[CrossRef](#)]
5. Vago, J.L.; Westall, F.; Coates, A.J.; Jaumann, R.; Korablev, O.; Ciarletti, V.; Mitrofanov, I.; Josset, J.-L.; De Sanctis, M.C.; Bibring, J.-P. Habitability on early Mars and the search for biosignatures with the ExoMars Rover. *Astrobiology* **2017**, *17*, 471–510. [[CrossRef](#)] [[PubMed](#)]
6. Webster, C.R.; Mahaffy, P.R.; Atreya, S.K.; Moores, J.E.; Flesch, G.J.; Malespin, C.; McKay, C.P.; Martinez, G.; Smith, C.L.; Martin-Torres, J.; et al. Background levels of methane in Mars’ atmosphere show strong seasonal variations. *Science* **2018**, *360*, 1093–1096. [[CrossRef](#)]
7. Oehler, D.Z.; Etioppe, G. Methane Seepage on Mars: Where to Look and Why. *Astrobiology* **2017**, *17*, 1233–1264. [[CrossRef](#)] [[PubMed](#)]
8. Ferry, J.G. How to Make a Living by Exhaling Methane. *Annu. Rev. Biochem.* **2010**, *64*, 453–473. [[CrossRef](#)]
9. Nixon, S.L.; Cousins, C.R.; Cockell, C.S. Plausible microbial metabolisms on Mars: Microbial metabolisms on Mars. *Astron. Geophys.* **2013**, *54*, 1.13–1.16. [[CrossRef](#)]
10. Holm, N.G.; Oze, C.; Mousis, O.; Waite, J.H.; Guilbert-Lepoutre, A. Serpentinization and the Formation of  $\text{H}_2$  and  $\text{CH}_4$  on Celestial Bodies (Planets, Moons, Comets). *Astrobiology* **2015**, *15*, 587–600. [[CrossRef](#)]
11. McMahan, S.; Parnell, J.; Blamey, N.J.F. Evidence for Seismogenic Hydrogen Gas, a Potential Microbial Energy Source on Earth and Mars. *Astrobiology* **2016**, *16*, 690–702. [[CrossRef](#)]
12. Blank, J.G.; Green, S.J.; Blake, D.; Valley, J.W.; Kita, N.T.; Treiman, A.; Dobson, P.F. An alkaline spring system within the Del Puerto Ophiolite (California, USA): A Mars analog site. *Planet. Space Sci.* **2009**, *57*, 533–540. [[CrossRef](#)]



13. Etiope, G.; Ehlmann, B.L.; Schoell, M. Low temperature production and exhalation of methane from serpentinized rocks on Earth: A potential analog for methane production on Mars. *Icarus* **2013**, *224*, 276–285. [[CrossRef](#)]
14. Alexander, W.R.; Milodowski, A.E. *Cyprus Natural Analogue Project (CNAP) Phase IV Final Report*; Nuclear Decommissioning Agency: Harwell, UK, 2015.
15. D’Alessandro, W.; Daskalopoulou, K.; Calabrese, S.; Bellomo, S. Water chemistry and abiogenic methane content of a hyperalkaline spring related to serpentinization in the Argolida ophiolite (Ermioni, Greece). *Mar. Pet. Geol.* **2018**, *89*, 185–193. [[CrossRef](#)]
16. Ramirez, R.M.; Craddock, R.A. The geological and climatological case for a warmer and wetter early Mars. *Nat. Geosci.* **2018**, *11*, 230–237. [[CrossRef](#)]
17. Hu, R.; Kass, D.M.; Ehlmann, B.L.; Yung, Y.L. Tracing the fate of carbon and the atmospheric evolution of Mars. *Nat. Commun.* **2015**, *6*, 10003. [[CrossRef](#)] [[PubMed](#)]
18. Horgan, B.H.N.; Anderson, R.B.; Dromart, G.; Amador, E.S.; Rice, M.S. The mineral diversity of Jezero crater: Evidence for possible lacustrine carbonates on Mars. *Icarus* **2020**, *339*, 113526. [[CrossRef](#)]
19. Burke, I.; Mortimer, R.; Palani, S.; Whittleston, R.; Lockwood, C.; Ashley, D.; Stewart, D. Biogeochemical reduction processes in a hyper-alkaline affected leachate soil profile. *Geomicrobiol. J.* **2012**, *29*, 769–779. [[CrossRef](#)]
20. Wormald, R.M.; Rout, S.P.; Mayes, W.; Gomes, H.; Humphreys, P.N. Hydrogenotrophic Methanogenesis under Alkaline Conditions. *Front. Microbiol.* **2020**, *11*, 614227. [[CrossRef](#)]
21. Rout, S.P.; Radford, J.; Laws, A.P.; Sweeney, F.; Elmekawy, A.; Gillie, L.J.; Humphreys, P.N. Biodegradation of the Alkaline Cellulose Degradation Products Generated during Radioactive Waste Disposal. *PLoS ONE* **2014**, *9*, e107433. [[CrossRef](#)]
22. Griffiths, R.I.; Whiteley, A.S.; O’Donnell, A.G.; Bailey, M.J. Rapid Method for Coextraction of DNA and RNA from Natural Environments for Analysis of Ribosomal DNA- and rRNA-Based Microbial Community Composition. *Appl. Environ. Microbiol.* **2000**, *66*, 5488–5491. [[CrossRef](#)]
23. Kral, T.A.; Birch, W.; Lavender, L.E.; Virden, B.T. Potential use of highly insoluble carbonates as carbon sources by methanogens in the subsurface of Mars. *Planet. Space Sci.* **2014**, *101*, 181–185. [[CrossRef](#)]
24. Phillips-Lander, C.M.; Parnell, S.R.; McGraw, L.E.; Madden, M.E.E. Carbonate dissolution rates in high salinity brines: Implications for post-Noachian chemical weathering on Mars. *Icarus* **2018**, *307*, 281–293. [[CrossRef](#)]
25. Zastro, A.M.; Glotch, T.D. Distinct carbonate lithologies in Jezero crater, Mars. *Geophys. Res. Lett.* **2021**, *48*, 9. [[CrossRef](#)] [[PubMed](#)]
26. Siegert, M.; Li, X.-F.; Yates, M.D.; Logan, B.E. The presence of hydrogenotrophic methanogens in the inoculum improves methane gas production in microbial electrolysis cells. *Front. Microbiol.* **2015**, *5*, 778. [[CrossRef](#)] [[PubMed](#)]
27. Maus, I.; Wibberg, D.; Stantscheff, R.; Cibis, K.; Eikmeyer, F.-G.; König, H.; Pühler, A.; Schlüter, A. Complete genome sequence of the hydrogenotrophic archaeon *Methanobacterium* sp. Mb1 isolated from a production-scale biogas plant. *J. Biotechnol.* **2013**, *168*, 734–736. [[CrossRef](#)] [[PubMed](#)]
28. Luo, Y.; Chen, H.; Yu, B.; He, J.; Zheng, P.; Mao, X.; Tian, G.; Yu, J.; Huang, Z.; Luo, J. Dietary pea fiber increases diversity of colonic methanogens of pigs with a shift from *Methanobrevibacter* to *Methanomassiliicoccus*-like genus and change in numbers of three hydrogenotrophs. *BMC Microbiol.* **2017**, *17*, 17. [[CrossRef](#)]
29. Maus, I.; Wibberg, D.; Stantscheff, R.; Eikmeyer, F.-G.; Seffner, A.; Boelter, J.; Szczepanowski, R.; Blom, J.; Jaenicke, S.; König, H. Complete genome sequence of the hydrogenotrophic, methanogenic archaeon *Methanoculleus bourgensis* strain MS2T, isolated from a sewage sludge digester. *Am. Soc. Microbiol.* **2012**, *194*, 19.
30. Lambie, S.C.; Kelly, W.J.; Leahy, S.C.; Li, D.; Reilly, K.; McAllister, T.A.; Valle, E.R.; Attwood, G.T.; Altermann, E. The complete genome sequence of the rumen methanogen *Methanosarcina barkeri* CM1. *Stand. Genom. Sci.* **2015**, *10*, 57. [[CrossRef](#)]
31. Ragsdale, S.W.; Pierce, E. Acetogenesis and the Wood–Ljungdahl pathway of CO<sub>2</sub> fixation. *Biochim. Biophys. Acta BBA Proteins Proteom.* **2008**, *1784*, 1873–1898. [[CrossRef](#)]
32. Borrel, G.; Adam, P.S.; Gribaldo, S. Methanogenesis and the Wood–Ljungdahl Pathway: An Ancient, Versatile, and Fragile Association. *Genome Biol. Evol.* **2016**, *8*, 1706–1711. [[CrossRef](#)]
33. Orange, F.; Westall, F.; Disnar, J.R.; Prieur, D.; Bienvenu, N.; Le Romancer, M.; Défarge, C. Experimental silicification of the extremophilic Archaea *Pyrococcus abyssi* and *Methanocaldococcus jannaschii*: Applications in the search for evidence of life in early Earth and extraterrestrial rocks. *Geobiology* **2009**, *7*, 403–418. [[CrossRef](#)]
34. Joseph, R.G.; Planchon, O.; Duxbury, N.S.; Latif, K.; Kidron, G.J.; Consorti, L.; Armstrong, R.A.; Gibson, C.; Schild, R. Oceans, Lakes, and Stromatolites on Mars. *Adv. Astron.* **2020**, *2020*, 6959532. [[CrossRef](#)]